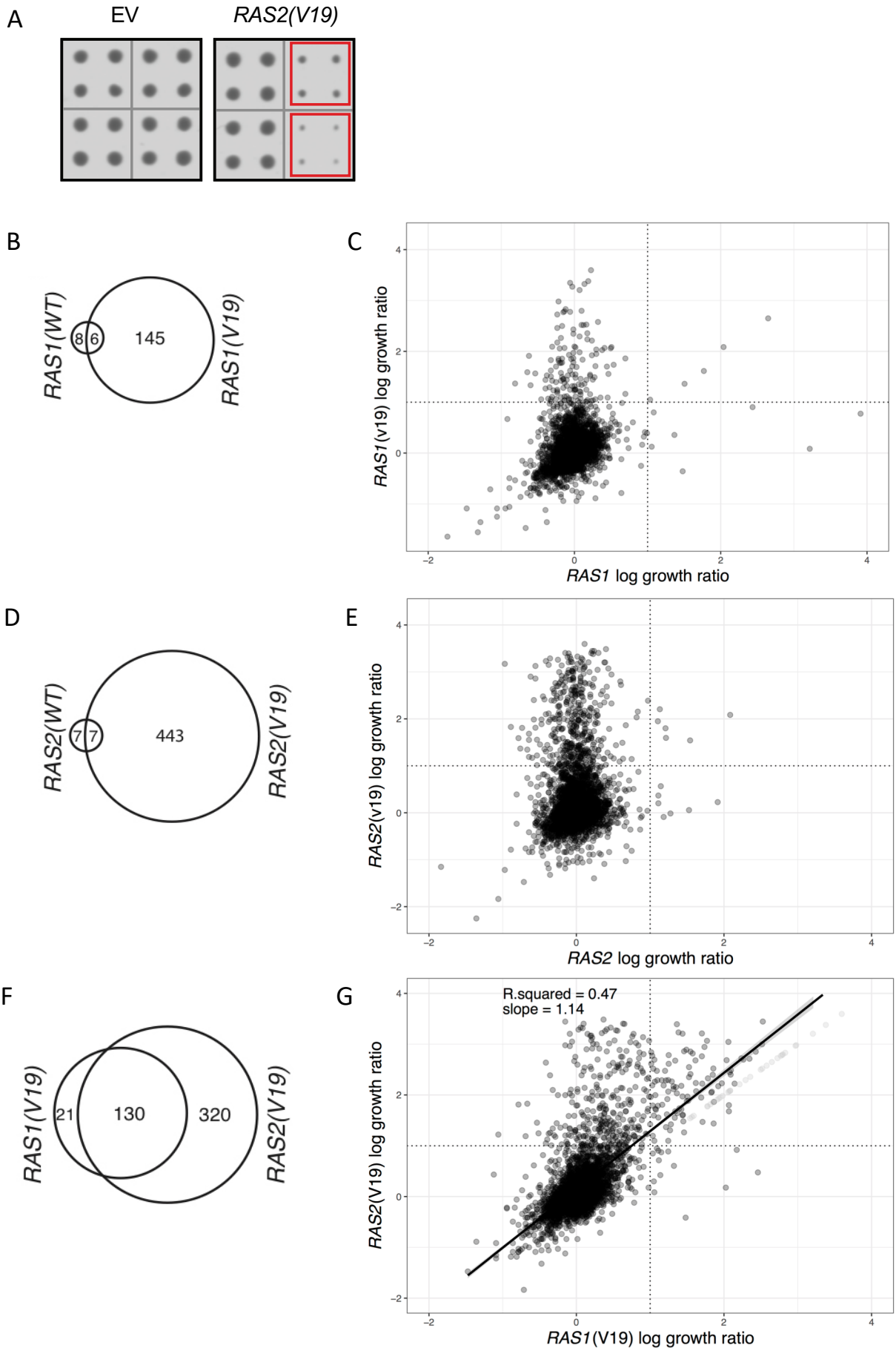
A
EV
RAS2(V19)
B
RAS1(WT)
RAS1(V19)
8
6
145
C
RAS1(v19) log growth ratio
RAS1 log growth ratio
D
RAS2(WT)
RAS2(V19)
7
7
443
E
RAS2(v19) log growth ratio
RAS2 log growth ratio
F
RAS1(V19)
RAS2(V19)
21
130
320
G
R.squared = 0.47
slope = 1.14
RAS2(V19) log growth ratio
RAS1(V19) log growth ratio

Figure S1. Genome-wide synthetic lethal screens with *RAS1(V19)* and *RAS2(V19)* identify overlapping sets of genes.

(A) Yeast strains containing the empty vector (EV) control (left) were used as a growth reference for the same strains expressing *RAS2(V19)* (right). Each of the ~4800 gene deletion strains is represented by 4 colonies. Two strains showing a growth defect in the presence of *RAS2(V19)* are outlined in red.

(B) Venn diagram showing the overlap between an SL screen with *RAS1* wild type (WT), that yielded 14 strains with a growth defect, and mutant *RAS1(V19)* screen that yielded 151 strains with a growth defect.

(C) Plot showing log growth ratios of the *RAS1* and *RAS1(V19)* SL screens. Ratios are calculated as the base 2 log of the growth ratio of the empty vector control divided by *RAS* plasmid, thus higher values represent slower growth when a *RAS* allele is expressed. Dotted lines show the 2-fold growth ratio difference from the population mean.

(D) Overlap between *RAS2* wild type (WT) screen and mutant *RAS2(V19)* screen.

(E) Plot of log growth ratios for the *RAS2* and *RAS2(V19)* SL screens.

(F) Venn diagram showing overlap between two screens with mutant *RAS*, *RAS1(V19)* and *RAS2(V19)*. 130 out of 151 total synthetic lethal interactions from the *RAS1(V19)* screen are also present in the *RAS2(V19)* screen.

(G) Plot of log growth ratios and correlation between the *RAS1(V19)* and *RAS2(V19)* screens. The slow growth phenotype in the population of deletion mutants was overall more severe in the *RAS2(V19)* screen as compared with the *RAS1(V19)* screen. The solid line indicates the calculated correlation (slope and R^2 value listed in inset). There are approximately 30 strains that show no growth with *RAS1*(V19) and *RAS2*(V19) and thus give identical growth ratios, i.e., slope = 1.0 (lighter gray points in the upper right quadrant).

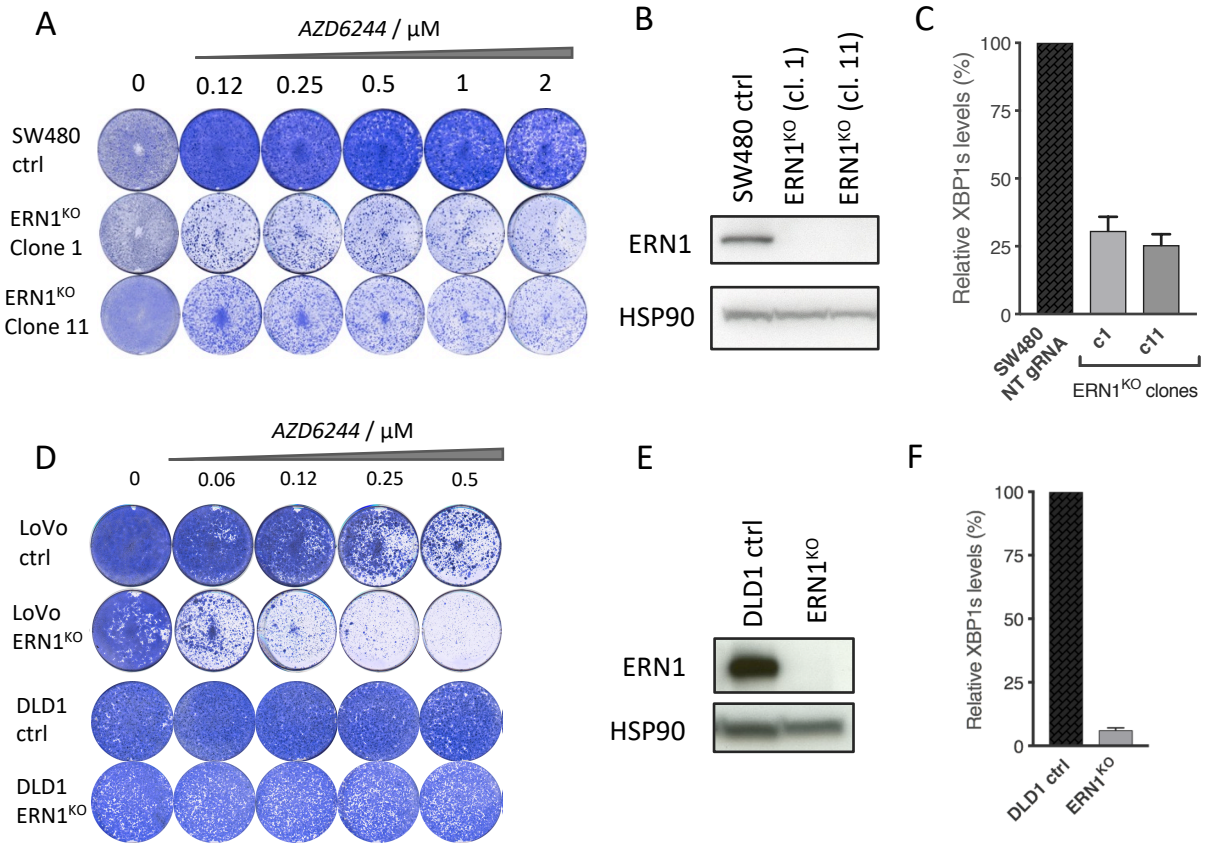

Figure S2. The response of SW480 *ERN1*^{KO} and DLD1 *ERN1*^{KO} *KRAS* mutant colon cancer cells to MEK inhibition.

(A) Colony formation assay of SW480 *ERN1*^{KO} cells in indicated concentrations of the MEK inhibitor AZD6244.

(B) The expression of ERN1 in SW480 *ERN1*^{KO} cells.

(C) Quantification of spliced XBP1 mRNA (XBP1s) in SW480 *ERN1*^{KO} clones.

(D) Colony formation assay of LoVo *ERN1*^{KO} cells and DLD1 *ERN1*^{KO} cells in indicated concentrations of the MEK inhibitor AZD6244.

(E) The expression of ERN1 in DLD1 *ERN1*^{KO} cells.

(F) Quantification of spliced XBP1 mRNA (XBP1s) in DLD1 *ERN1*^{KO} clone.

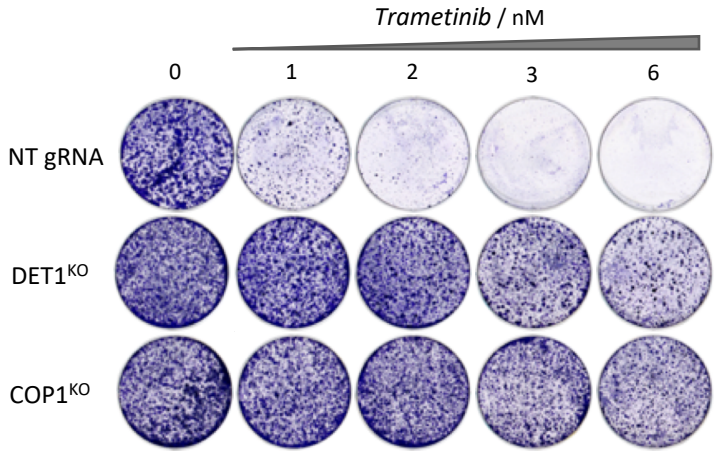

Figure S3. Colony formation assays of *DET1* and *COP1* knockout cells (in LoVo *ERN1*^{KO} background) in the presence and absence of the MEK inhibitor trametinib are shown relative to control cells expressing non-targeting (NT) gRNA.

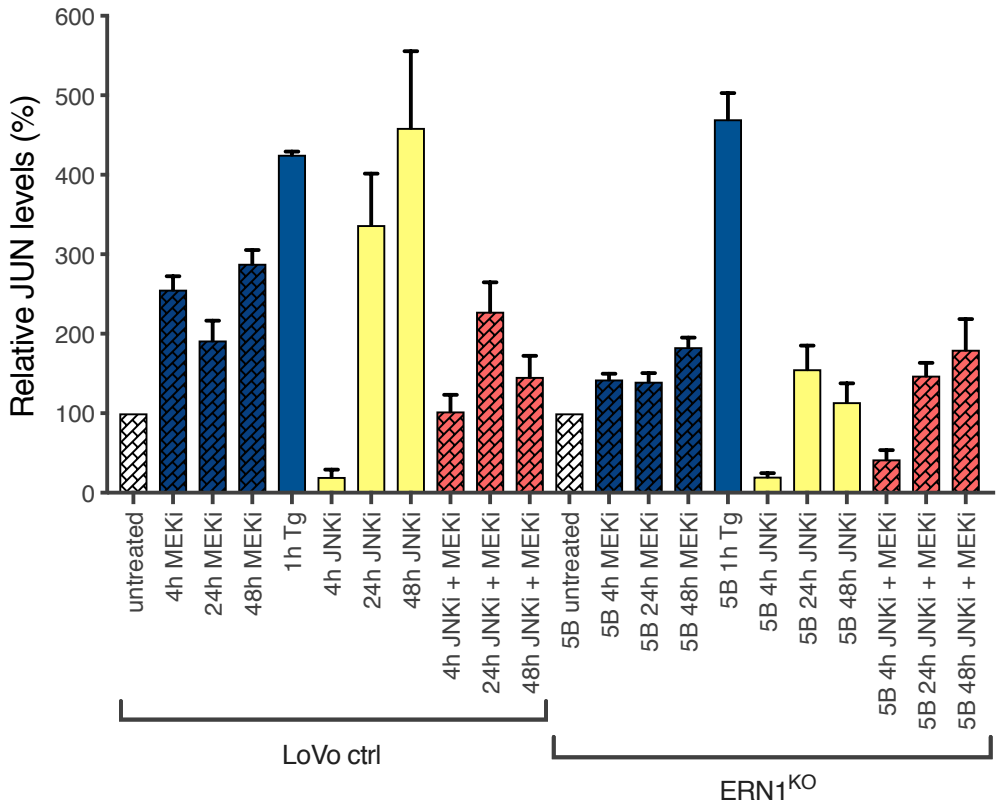

Figure S4. Quantification of JUN expression levels in MEK inhibitor (MEKi, 1 μM AZD6244), JNK inhibitor (JNKi, 1 μM SR-3306) and combination treatment (JNKi + MEKi). One hour thapsigargin treatment (Tg, 100 nM) was used as a control. Error bars represent standard deviation of three replicate experiments.

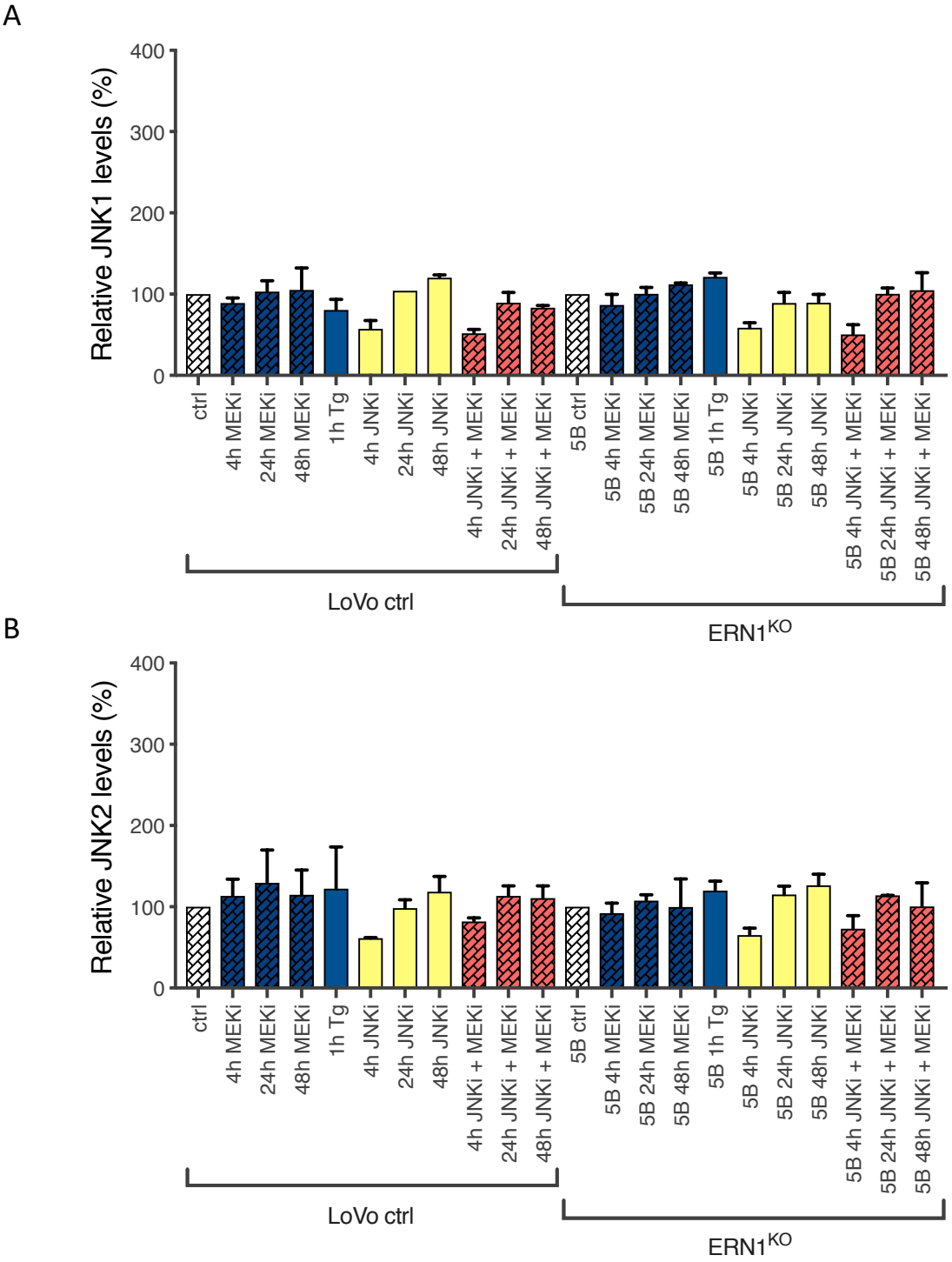

Figure S5. Quantification of JNK1 (A) and JNK2 (B) expression levels in MEK inhibitor (MEKi, 1 μM AZD6244), JNK inhibitor (JNKi, 1 μM SR-3306) and combination treatment (JNKi + MEKi). One hour thapsigargin treatment (Tg, 100 nM) was used as a control. Error bars represent standard deviation of three replicate experiments.